A stretchable slippery surface fabricated by femtosecond laser direct writing ⊘

Special Collection: Superhydrophobic Surfaces

Jialiang Zhang; Qing Yang ✉; Qingyun Ma (iD) ; Fangzheng Ren; Haoyu Li; Chengjun Zhang; Yang Cheng; Feng Chen ✉ (iD)

Check for updates

CrossMark

View Online

Export Citation

A stretchable slippery surface fabricated by femtosecond laser direct writing

View Online   Export Citation   CrossMark

Jialiang Zhang,[1] Qing Yang,[2,a)] Qingyun Ma,[1] (iD) Fangzheng Ren,[1] Haoyu Li,[1] Chengjun Zhang,[2] Yang Cheng,[2] and Feng Chen[1,a)] (iD)

AFFILIATIONS

[1]State Key Laboratory for Manufacturing System Engineering and Shaanxi Key Laboratory of Photonics Technology for Information, School of Electronic Science and Engineering, Xi'an Jiaotong University, Xi'an 710049, People's Republic of China
[2]School of Mechanical Engineering, Xi'an Jiaotong University, Xi'an 710049, People's Republic of China

Note: This paper is part of the APL Special Collection on Superhydrophobic Surfaces.
[a)]Authors to whom correspondence should be addressed: yangqing@mail.xjtu.deu.cn and chenfeng@mail.xjtu.edu.cn

ABSTRACT

Surface conditions of flexible electronic devices can affect their accuracy, so it is necessary to keep surfaces clean and stable to ensure their correct-long-term operation. The Nepenthes-inspired slippery surface has excellent self-cleaning, stability, and self-healing properties. A slippery surface with stretching durability is significant for application to a flexible sensors surface. As an advanced micro-nanomanufacturing method, femtosecond laser has become an effective method for preparing porous structures to process a slippery surface. In this study, a femtosecond laser was used to prepare an interconnected porous structure on pre-stretched polydimethylsiloxane in one step. The slippery surface was prepared after being infused with lubricant, which maintained the slippery performance under tensile conditions and after hundreds of stretch cycles. Moreover, it exhibits remarkable self-cleaning and chemical stability. This stretchable slippery surface prepared by femtosecond laser direct writing presents good prospects for flexible electronic devices that require a stable surface in various extreme environmental applications.

The surfaces of flexible electronic devices are affected by conditions, such as stretching and fouling in various extreme environments.[1–3] While being affected by these factors, it is necessary to keep the surface clean to maintain sensitivity of the sensor. A slippery liquid infused porous surface (SLIPS) can provide a stable lubricant surface with great self-cleaning and self-healing performance.[4–9] In current SLIPS development, the porous structure of the surface is very important in maintaining the lubricant layer that provides the slippery performance.[10–12] However, when the surface suffers tensile, bending, or other deformations, the porous structure of the SLIPS is easily damaged; thus, the lubricant is extruded, which limits its slippery properties.[13,14]

The porous structure of the SLIPS plays a key role in storing the lubricant, so the stability of the porous structure is closely related to SLIPS stability.[15] Current research focuses on the development of SLIPS based on hard matrix materials, including metals and glass.[16,17] The porous structure on these hard materials is also a rigid structure, which cannot be deformed or stretched. The SLIPS of polymer materials is usually a slippery surface coating or cannot be stretched. While

the coating itself may possess flexibility, it is necessary to adhere it to a solid substrate surface. However, the tensile strain experienced by each layer may not be perfectly aligned. These factors limit the application of slippery surfaces in deformation conditions, especially in flexible electronic devices. Che *et al.* prepared a flexible slippery surface by mixing a MoS_2 nanonetwork with polydimethylsiloxane (PDMS).[18] After multiple repetitions of bending and stretching, it still maintained a certain slippery performance and excellent self-cleaning function. Wang *et al.* coated a copolymer on a substrate material.[19] By pouring perfluoropolyether into the coating, a flexible slippery surface was achieved, which also exhibited good tensile, bending properties, and liquid resistance. These flexible slippery surfaces were prepared by chemical methods, for which the preparation process is complicated and the heterogeneous materials have the risk of detachment in long-term use. In the present research, femtosecond laser micro-nano processing serves as an advanced manufacturing method that offers high processing accuracy, excellent controllability, and wide versatility. It possesses a distinct advantage in fabrication of highly wettable surfaces and has successfully created numerous types of such surfaces.[20] As

a widely used elastic material, PDMS has excellent flexibility and stretchability, making it a prominent matrix material in flexible electronic research. By employing femtosecond laser direct writing technology, it becomes possible to directly fabricate superhydrophobic surfaces on PDMS with micro-nano composite structures in a single step. Consequently, if the same femtosecond laser can be utilized to create interconnected porous structures on PDMS, there is optimistic anticipation for the facile preparation of a stretchable slippery surface using this advanced manufacturing method.[21,22]

In this study, a stretchable slippery surface was prepared by femtosecond laser ablation and lubricant infusion. By adjusting the laser power and repetition frequency, an interconnected porous structure could be prepared in one step on the surface of pre-stretched PDMS. The porous PDMS showed excellent superhydrophobic properties before and after stretching. The contact angle (CA) exceeded 150° and the sliding angle (SA) was less than 3°. Infusion of an interconnected porous structure with lubricant gave a stretchable slippery surface. This stretchable slippery surface that was processed by pre-stretching to an extent of 40% maintained good slippery performance even after 600 continuous stretching cycles. Various composite liquids could easily slip off the surface, including milk, tomato juice, coffee, and droplets of various pH values. This stretchable slippery surface was fabricated on a surface of flexible electronic sensor, which endows the flexible sensor with good self-cleaning properties.

The PDMS (size: 4×2 cm^2, thickness: 500 μm) pre-stretched to a certain length and fixed on a two-dimensional translation stage. The femtosecond laser parameters include a laser power of 217 mW and a repeated frequency of 1.67 kHz are selected. The laser is focused on the surface of the pre-stretched PDMS through a lens (f = 120 mm). The two-dimensional stage is programmed to move, so that the laser performs line scanning on the sample surface. After processing, silicone oil (100 mPa s) was dropped on the surface of the sample. The surface morphology of the stretchable slippery surface was observed by an optical microscope and an electron microscope (FlexSEM1000, HITACHI, Japan). The contact angle measuring instrument tests the contact angle and sliding angle (JC2000D, Powereach, China) and a multifunctional tension/compression testing system for testing the stretch cycle (ZQ-990B, ZHIQU, China).

The preparation method of the stretchable slippery surface was shown in Fig. 1(a). After the PDMS material was pre-stretched, the femtosecond laser ablated the interconnected porous structure on the PDMS surface in its stretched state. Pre-stretching refers to stretching the PDMS to different lengths and holding it until laser ablation process was completed. A lubricant was infused into the porous structure to obtain a stretchable slippery surface. The single pulse energy of femtosecond laser is 130 μJ and the pulse width is 263 fs. The speed of laser scanning and the distance between adjacent scanning lines are controlled by a mechanical mobile platform, which is 15 mm·s^{-1} and
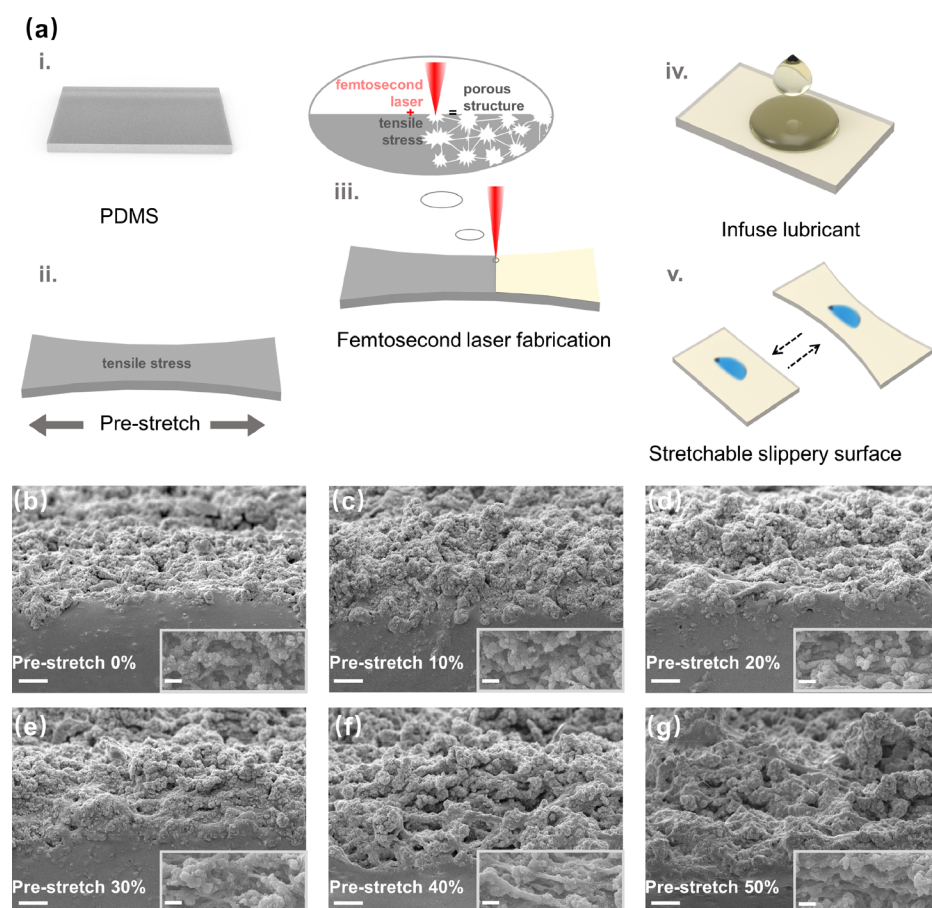

FIG. 1. (a) Fabrication process of stretchable SLIPS. (b)–(g) Cross-sectional microstructure with the pre-stretch rate of 0%–50%, the top view morphology in the small box. Scale bar:10 μm.

50 μm, respectively. Six groups of pre-stretching rates, ranging from 0% to 50%, were processed under the same laser parameters. These showed different microstructures, including cross-sectional and top views [Figs. 1(b)–1(g)]. In pre-stretched PDMS, the femtosecond laser can directly ablate interconnected porous structures on the surface, which differs from micro-nanostructures ablated under normal conditions. When the pre-stretching rate was 0% (i.e., unstretched), the PDMS was ablated in its original state, so the surface was only affected by femtosecond laser and consequently generated a uniform micro-nano rough structure.[23] When the pre-stretching rate exceeded 0%, the surface began to appear as an interconnected porous structure after femtosecond laser ablation, and the thickness of structure correspondingly increased.

The interconnected porous structure results from multi-physical field coupling on the PDMS surface. When the power density of a femtosecond laser pulse exceeds the damage threshold of the PDMS surface, it triggers nonlinear effects, such as multiphoton and avalanche ionization. Electrons on the PDMS surface absorb the laser energy, resulting in the formation of a high-pressure, high-temperature plasma above the surface. This plasma is also influenced by the pre-stretched surface stress. The synergistic effect of nonlinear effects and surface stress leads to formation of an interconnected porous structure on the PDMS surface as the plasma expands beyond it.[24,25] During the laser ablation process, the area exposed to the femtosecond laser instantly transforms to a melted state, resulting in generation of a gas-ejection surface. The molten state undergoes deformation due to internal stress in the pre-stretched PDMS. As the translation stage of sample moves and the focal point continues to shift, the deformed molten state rapidly cools and solidifies. The ejected gas also impacts the deformed molten state. Through the combined action of multi-physical fields, the femtosecond laser can directly create interconnected porous structures on a pre-stretched PDMS surface in a single step.

Femtosecond laser processing of pre-stretched PDMS also increases the thickness of the structure. When PDMS is in a pre-stretched state, its thickness reduces. Upon completion of the ablation, as the PDMS returns to its normal state, the thickness increases. Simultaneously, the porous structure on the surface contracts and compresses as the PDMS recovers from the stretched state to its normal state; thickness of the porous structure consequently increases. Therefore, when femtosecond laser ablates pre-stretched PDMS, it not only generates porous structures but also increases the thickness of these structures. Varying the pre-stretching rate changes the stress on the PDMS surface, consequently affecting the results of the multi-physical field, specifically the porous morphology of the surface.

With the increase in the pre-stretching rate, an interconnected porous structure started to appear, at first more densely and then sparsely [Figs. 1(b)–1(g)]. At 40% pre-stretching, the combined action of multi-physical fields produced the densest porous structure on the PDMS surface [Fig. 1(f)]. The cross section morphology shows that this structure thickest of the six samples, which means that it could store the most lubricant.

All six samples exhibited superhydrophobic properties following femtosecond laser ablation. The contact angle (CA) for all samples exceeded 150°, while the rolling-off angle remained below 3°. Interestingly, the superhydrophobic wettability demonstrated minimal change during sample stretching [Figs. 2(a) and 2(b)]. The reason for
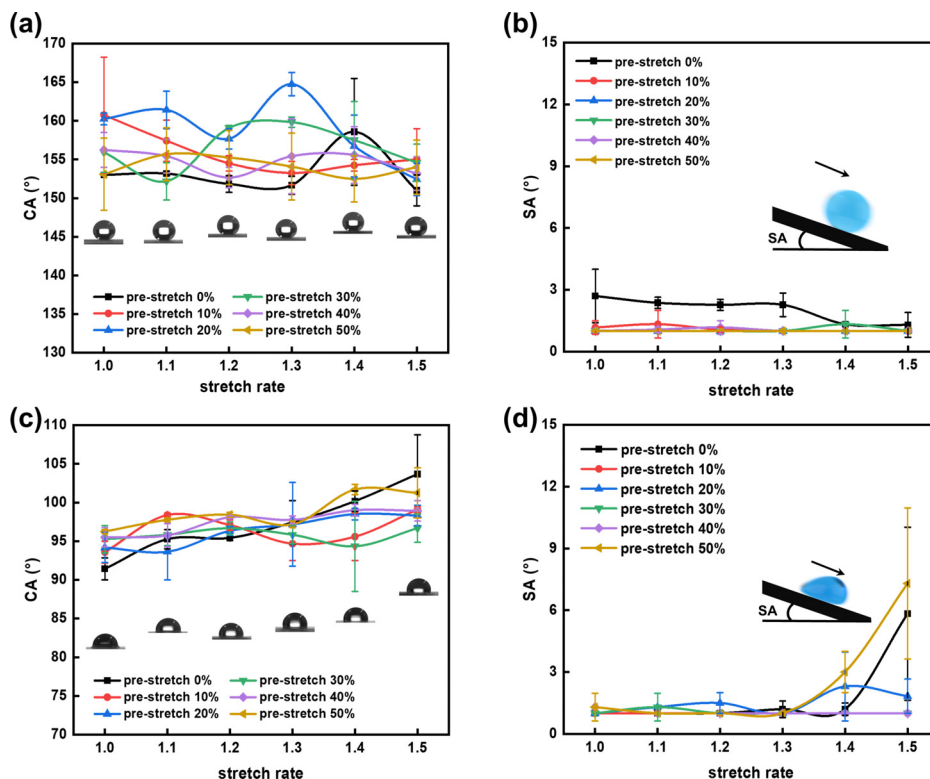

FIG. 2. (a) and (b) CA and SA with the stretching length increase in PDMS after femtosecond laser ablation with different pre-stretch extents. (c) and (d) CA and SA with the stretching length increase in slippery surface with different pre-stretched during stretch, 7 μl droplet.
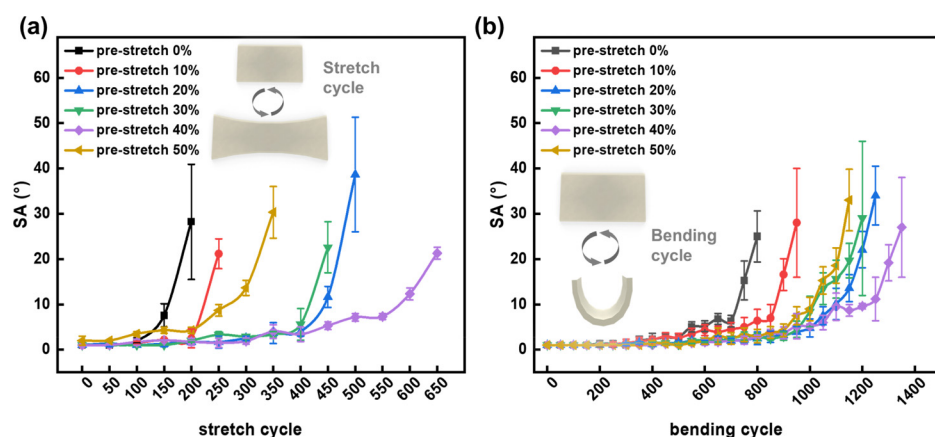
FIG. 3. (a) SA with the stretching cycles of slippery surfaces with different pre-stretching rates. (b) SA with the bending cycles of slippery surfaces with different pre-stretching rates.

the consistent superhydrophobic properties of these six samples lies in their micro-nanostructures, irrespective of whether the sample was in a normal or a stretched state. The combination of abundant micro-nanostructures and the inherently low surface energy of PDMS allow droplets to adopt a Cassie state on the surface.[26] The properties of superhydrophobic PDMS surface prepared by femtosecond laser ablation have been extensively explored in previous studies.[27,28] Corresponding slippery surfaces were obtained by infusing lubricant into the microstructures of PDMS, according to the rules for the preparation of a SLIPS.[29,30] The CA of the six slippery surfaces was approximately 95° without stretching and the SA was about 1°. When the samples were stretched to different lengths, the slippery surface in the stretched state showed different CA values; the CA increased by an average of 5° when these slippery surfaces were held at an 1.5 stretching rate.

The slippery surfaces prepared with pre-stretching extents of 0% and 50% had the largest CA value when held at 1.5 stretching extents, and the SA of the two samples increased from 1° to 6° during the stretching process [Figs. 2(c) and 2(d)]. According to the morphology, when the pre-stretching rate was 0% and 50%, only a very limited amount of lubricant could be stored owing to the very thin and sparse porous structure. In the stretched state, the lubricant is also easily lost. The greater the extent of stretch, the greater was the loss of lubricant, which revealed the more micro-nanostructure, resulting in an increase in CA. When the pre-stretching extents were 0% and 50%, the slippery performance of the prepared slippery surface reduced after stretching, and the droplets had a tendency to pin on the surface. The SA of other pre-stretched samples did not change much in either the stretched or unstretched state and were typically approximately 1°. These results show that the slippery surface prepared by femtosecond laser could maintain good slippery performance in the stretched state when the pre-stretching extent ranged from 10% to 40%. The interconnected porous structure retained the lubricant in both the stretched and unstretched states.

Applications of flexible electronic devices often encounter repeated stretching and bending scenarios. To assess their stretch durability, samples were prepared using six different extents of pre-stretching. Each sample was stretched by 50%, and the SA characterized every 50 cycles until the droplets could no longer slide. As the stretching cycle increased, the SA of the six slippery surfaces gradually

increases [Fig. 3(a)]. The samples have different densities and thickness of the interconnected porous structure, which influenced the amount of lubricant that could be stored. The lubricant loss experienced during the stretching cycle and droplet sliding on slippery surfaces with different pre-stretch extents affected the SA values. Based on the results of stretching durability characterization, the slippery surface with 40% pre-stretch extents demonstrated the best stretching durability performance, maintaining an SA below 10° after 600 stretch cycles.
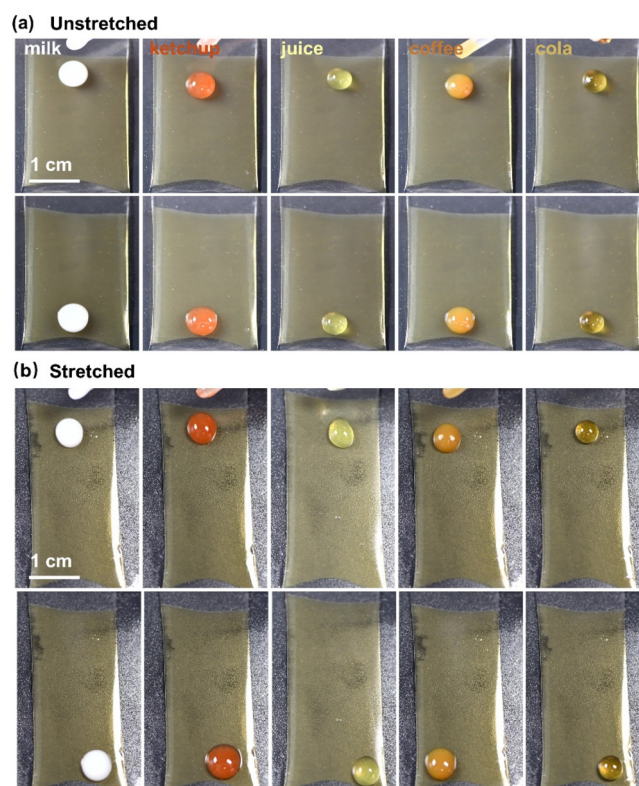

FIG. 4. (a) and (b) Composite liquids resistance of stretchable slippery surface before and after stretching.
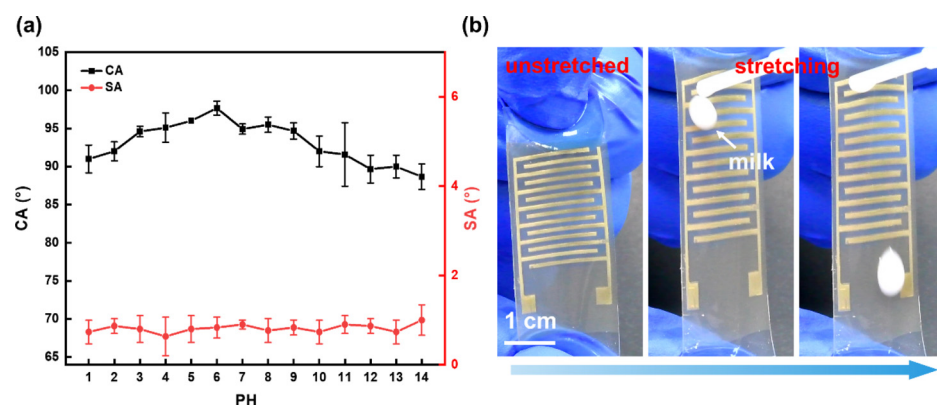
FIG. 5. (a) CA and SA of different pH value droplets on stretchable slippery surface. (b) Stretchable slippery surface on a flexible sensor surface.

This is attributed to the 40% pre-stretched slippery surface having the densest and thickest porous structure, enabling it to store the most lubricant and retain it within the structure without loss during hundreds of stretching cycles. In contrast, the unstretched slippery surface prepared by femtosecond laser ablation on unstretched PDMS, resulted in a micro-nanostructure, rather than a porous structure, for which the stretch cycles were limited to 200 and SA rapidly increased with the number of stretching cycles increase. The stretch cycles of other slippery surfaces failed in droplet sliding after hundreds of repetitions, with the number of stretching cycles ranging between 250 and 500. This is attributed to their porous structures; however, due to the lower density and thickness of these porous structures compared with the 40% pre-stretched structure, the lubricant decreased accordingly, consequently decreasing the number of stretching cycles.

Regarding the bending cycles, all six slippery surfaces demonstrated the ability to withstand hundreds of bending cycles without losing their slippery performance [Fig. 3(b)]. In comparison to the stretching cycle test, the bending test induces less variation in internal stress on the slippery surface, making it more quantities of bending cycle numbers. However, the number of bending tests is also influenced by the amount of stored lubricant. Based on previous findings, the slippery surface with a 40% pre-stretching rate can store the highest amount of lubricant, resulting in the best bending durability. This surface maintained a SA of less than 10° even after 1300 bending cycles.

In addition to water droplets, we also characterized the slippery performance of the stretchable slippery surface with many composite droplets before and after stretching, including milk, tomato sauce, juice, coffee, and cola (Fig. 4). Regardless of the state of the stretchable slippery surface, these composite droplets could easily slide away on the surface without leaving any trace. The excellent liquid resistance and self-cleaning properties of the stretchable slippery surface are of great significance to surface of flexible electronic devices.

The chemical stability of stretchable slippery surface was tested by droplets with different pH values. Solution of different pH values was prepared by mixing NaOH and H_2SO_4 solutions. The CA of different pH droplets on the stretchable slippery surfaces was 89°–95°. The CA decreased for pH values larger or smaller than 7. The reason is that the surface tension of the droplet decreased as the pH value changed from 7, thus lowering the CA. The SA values for all droplets were about 1°, which means the slippery performances of liquids with different pH values were similar. A stretchable slippery surface with good chemical stability was processed on a flexible sensor surface

[Fig. 5(b)]. The composite liquids easily slide away from the surface. The self-cleaning property of the stretchable slippery surface endows the flexible sensor surface with the same performance, which not only enables the sensor to be applied in more scenarios but also improves its service life.

In this study, a stretchable slippery surface was fabricated by femtosecond laser direct writing on a pre-stretched PDMS substrate. The stretchable slippery surface consisted of an interconnected porous structure on the PDMS surface and lubricant infusion. The interconnected porous structure of PDMS exhibited remarkable superhydrophobic properties, whether stretched or not. By infusing the lubricant into the interconnected porous structure, the resulting stretchable slippery surface exhibited excellent stretching durability and self-cleaning properties. The slippery surface processed with 40% pre-stretching extent of PDMS maintained its superior slippery performance even after 600 consecutive stretching cycles. Various composite liquids can easily slide off the surface, both with and without surface stretching. Owing to its exceptional stretch durability and self-cleaning properties, this slippery surface holds great potential for broadening the range of applications of flexible electronic devices.

AUTHOR DECLARATIONS
Conflict of Interest

The authors have no conflicts to disclose.

Author Contributions

Jialiang Zhang: Conceptualization (equal); Data curation (lead); Investigation (lead); Methodology (lead); Writing – original draft (lead). **Qing Yang:** Funding acquisition (equal); Methodology (equal); Project administration (equal). **Qingyun Ma:** Investigation (equal); Methodology (supporting). **Fangzheng Ren:** Methodology (supporting). **Haoyu Li:** Investigation (equal); Methodology (supporting). **Chengjun Zhang:** Conceptualization (supporting); Validation (supporting). **Yang Cheng:** Investigation (supporting). **Feng Chen:** Funding acquisition (equal); Project administration (equal); Supervision (equal); Writing – review & editing (equal).

DATA AVAILABILITY

The data that support the findings of this study are available from the corresponding authors upon reasonable request.

REFERENCES

[1]M. M. Rodgers, V. M. Pai, and R. S. Conroy, "Recent advances in wearable sensors for health monitoring," IEEE Sens. J. **15**(6), 3119–3126 (2015).

[2]S. J. Kim, K. Choi, B. Lee, Y. Kim, and B. H. Hong, "Materials for flexible, stretchable electronics: graphene and 2D materials," Annu. Rev. Mater. Res. **45**(1), 63–84 (2015).

[3]C. Zhang, Z. Li, H. Li, Q. Yang, H. Wang, C. Shan, J. Zhang, X. Hou, and F. Chen, "Femtosecond laser-induced supermetalphobicity for design and fabrication of flexible tactile electronic skin sensor," ACS Appl. Mater. Interfaces **14**(33), 38328–38338 (2022).

[4]M. A. Samaha and M. Gad-el-Hak, "Slippery surfaces: A decade of progress," Phys. Fluids **33**(7), 071301 (2021).

[5]F. Chen, Y. Wang, Y. Tian, D. Zhang, J. Song, C. R. Crick, C. J. Carmalt, I. P. Parkin, and Y. Lu, "Robust and durable liquid-repellent surfaces," Chem. Soc. Rev. **51**(20), 8476–8583 (2022).

[6]Y. Wang, J. Meng, and S. Wang, "Recent progress of bioinspired scalephobic surfaces with specific barrier layers," Langmuir **37**(29), 8639–8657 (2021).

[7]W. Yan, S. Xue, B. Xiang, X. Zhao, W. Zhang, P. Mu, and J. Li, "Recent advances of slippery liquid-infused porous surfaces with anti-corrosion," Chem. Commun. **59**, 2182 (2023).

[8]W. Yao, L. Wu, L. Sun, B. Jiang, and F. Pan, "Recent developments in slippery liquid-infused porous surface," Prog. Organic Coat. **166**, 106806 (2022).

[9]L. Chen, S. Huang, R. H. A. Ras, and X. Tian, "Omniphobic liquid-like surfaces," Nat. Rev. Chem. **7**(2), 123–137 (2023).

[10]H. Xiang, Y. Yuan, C. Zhang, X. Dai, T. Zhu, L. Song, Y. Gai, and R. Liao, "Key factors affecting durable anti-icing of slippery surfaces: Pore size and porosity," ACS Appl. Mater. Interfaces **15**(2), 3599–3612 (2023).

[11]L. Hao, R. Jiang, J. Gao, J. Xu, L. Tian, X. Zhang, S. Zhou, J. Zhao, and L. Ren, "Metal-organic framework (MOF)-based slippery liquid-infused porous surface (SLIPS) for purely physical antibacterial applications," Appl. Mater. Today **27**, 101430 (2022).

[12]C. Sung and Y. Heo, "Porous layer-by-layer films assembled using polyelectrolyte blend to control wetting properties," Polymers **13**(13), 2116 (2021).

[13]H. Tran, Y. Kim, C. Ternon, M. Langlet, D. Riassetto, and D. Lee, "Lubricant depletion-resistant slippery liquid-infused porous surfaces via capillary rise lubrication of nanowire array," Adv. Mater. Interfaces **8**(7), 2002058 (2021).

[14]Y. Fang, J. Yong, Y. Cheng, Q. Yang, X. Hou, and F. Chen, "Liquid-infused slippery stainless steel surface prepared by alcohol-assisted femtosecond laser ablation," Adv. Mater. Interfaces **8**(5), 2001334 (2021).

[15]Q. Yang, Y. Cheng, Z. Fang, J. Zhang, X. Hou, and F. Chen, "The preparation and applications of bio-inspired slippery surface by femtosecond laser micro-nano manufacturing," Opto-Electron. Eng. **49**(1), 210326 (2022).

[16]P. Zhang, H. Chen, L. Zhang, Y. Zhang, D. Zhang, and L. Jiang, "Stable slippery liquid-infused anti-wetting surface at high temperatures," J. Mater. Chem. A **4**(31), 12212–12220 (2016).

[17]M. Yu, M. Liu, Y. Hou, S. Fu, L. Zhang, M. Li, and D. Wang, "Covalently grafted liquids for transparent and omniphobic surfaces via thiol-ene click chemistry," J. Mater. Sci. **55**(27), 12811–12825 (2020).

[18]P. Che, X. Han, P. Guo, X. Wang, S. Cheng, K. Han, L. Jiang, and L. Heng, "Robust yet flexible slippery layered composite surfaces with a programmable pressure-resistance response under extreme environmental conditions," J. Mater. Chem. A **10**(28), 14933–14942 (2022).

[19]Y. Wang, B. Qian, C. Lai, X. Wang, K. Ma, Y. Guo, X. Zhu, B. Fei, and J. H. Xin, "Flexible slippery surface to manipulate droplet coalescence and sliding, and its practicability in wind-resistant water collection," ACS Appl. Mater. Interfaces **9**(29), 24428–24432 (2017).

[20]J. Yong, Q. Yang, X. Hou, and F. Chen, "Nature-inspired superwettability achieved by femtosecond lasers," Ultrafast Sci. **2022**, 9895418.

[21]M. Li, T. Yang, Q. Yang, Z. Fang, H. Bian, C. Zhang, X. Hou, and F. Chen, "Bioinspired anti-fogging and anti-fouling artificial compound eyes," Adv. Opt. Mater. **10**(17), 2200861 (2022).

[22]X. Bai, X. Gou, J. Zhang, J. Liang, L. Yang, S. Wang, X. Hou, and F. Chen, "A review of smart superwetting surfaces based on shape-memory micro/nano-structures," Small **19**(15), 2206463 (2023).

[23]J. Yong, F. Chen, Q. Yang, D. Zhang, G. Du, J. Si, F. Yun, and X. Hou, "Femtosecond laser weaving superhydrophobic patterned PDMS surfaces with tunable adhesion," J. Phys. Chem. C **117**(47), 24907–24912 (2013).

[24]J. Yong, F. Chen, Q. Yang, U. Farooq, H. Bian, G. Du, and X. Hou, "Controllable underwater anisotropic oil-wetting," Appl. Phys. Lett. **105**(7), 071608 (2014).

[25]F. Chen, D. Zhang, Q. Yang, J. Yong, G. Du, J. Si, F. Yun, and X. Hou, "Bioinspired wetting surface via laser microfabrication," ACS Appl. Mater. Interfaces **5**(15), 6777–6792 (2013).

[26]A. Cassie and S. Baxter, "Wettability of porous surfaces," Trans. Faraday Soc. **40**(1), 546–551 (1944).

[27]J. Yong, F. Chen, Q. Yang, J. Huo, and X. Hou, "Superoleophobic surfaces," Chem. Soc. Rev. **46**(14), 4168–4217 (2017).

[28]J. Yong, F. Chen, M. Li, Q. Yang, Y. Fang, J. Huo, and X. Hou, "Remarkably simple achievement of superhydrophobicity, superhydrophilicity, underwater superoleophobicity, underwater superoleophilicity, underwater superaerophobicity, and underwater superaerophilicity on femtosecond laser ablated PDMS surfaces," J. Mater. Chem. A **5**(48), 25249–25257 (2017).

[29]T.-S. Wong, S. H. Kang, S. K. Y. Tang, E. J. Smythe, B. D. Hatton, A. Grinthal, and J. Aizenberg, "Bioinspired self-repairing slippery surfaces with pressure-stable omniphobicity," Nature **477**(7365), 443–447 (2011).

[30]Y. Fang, J. Yong, J. Huo, Q. Yang, Y. Cheng, J. Liang, and F. Chen, "Bioinspired slippery surface fabricated by femtosecond laser and its applications," Laser Optoelectron. Prog. **57**(11), 111413 (2020).